Journal of the American Heart Association

ORIGINAL RESEARCH

Increased Lung Uric Acid Deteriorates Pulmonary Arterial Hypertension

Takanori Watanabe, MD; Mariko Ishikawa, MD, PhD; Kohtaro Abe (iD), MD, PhD; Tomohito Ishikawa, MD; Satomi Imakiire, MD; Kohei Masaki (iD), MD; Kazuya Hosokawa, MD, PhD; Tomoko Fukuuchi (iD), PhD; Kiyoko Kaneko, PhD; Toshio Ohtsubo, MD, PhD; Mayumi Hirano (iD), PhD; Katsuya Hirano, MD, PhD; Hiroyuki Tsutsui, MD, PhD

BACKGROUND: Recent studies have demonstrated that uric acid (UA) enhances arginase activity, resulting in decreased NO in endothelial cells. However, the role of lung UA in pulmonary arterial hypertension (PAH) remains uncertain. We hypothesized that increased lung UA level contributes to the progression of PAH.

METHODS AND RESULTS: In cultured human pulmonary arterial endothelial cells, voltage-driven urate transporter 1 (URATv1) gene expression was detected, and treatment with UA increased arginase activity. In perfused lung preparations of VEGF receptor blocker (SU5416)/hypoxia/normoxia-induced PAH model rats, addition of UA induced a greater pressure response than that seen in the control and decreased lung cGMP level. UA-induced pressor responses were abolished by benzbromarone, a UA transporter inhibitor, or L-norvaline, an arginase inhibitor. In PAH model rats, induction of hyperuricemia by administering 2% oxonic acid significantly increased lung UA level and induced greater elevation of right ventricular systolic pressure with exacerbation of occlusive neointimal lesions in small pulmonary arteries, compared with nonhyperuricemic PAH rats. Administration of benzbromarone to hyperuricemic PAH rats significantly reduced lung UA levels without changing XOR (xanthine oxidoreductase) activity, and attenuated right ventricular systolic pressure increase and occlusive lesion development. Topiroxostat, a XOR inhibitor, significantly reduced lung XOR activity in PAH rats, with no effects on increase in right ventricular systolic pressure, arterial elastance, and occlusive lesions. XOR-knockout had no effects on right ventricular systolic pressure increase and arteriolar muscularization in hypoxia-exposed mice.

CONCLUSIONS: Increased lung UA per se deteriorated PAH, whereas XOR had little impact. The mechanism of increased lung UA may be a novel therapeutic target for PAH complicated with hyperuricemia.

Key Words: arginase ■ pulmonary arterial hypertension ■ URATv1 ■ uric acid ■ xanthine oxidoreductase

Pulmonary arterial hypertension (PAH) is a diverse group of diseases characterized by narrowing of small pulmonary arteries and arterioles, resulting in increased pulmonary vascular resistance and pressure.[1] The major factors contributing to the vascular narrowing are sustained vasoconstriction and structural remodeling, including small pulmonary arterial medial thickening, occlusive neointimal, and complex plexiform lesions.[2,3] Despite recent advances in treatment, the prognosis of advanced PAH remains poor.[4]

Therefore, the development of a therapeutic strategy targeting a novel molecule is urgently needed.

Serum uric acid (UA) level correlates positively with mean pulmonary arterial pressure, disease severity, and prognosis in patients with PAH,[5–7] but little is known about its pathologic role in PAH. A study showed that UA decreased NO release from porcine pulmonary arterial endothelial cells (PAECs) by activating arginase to degrade L-arginase a substrate of NO, and arginase inhibition abolished UA-induced inhibition of

JAHA is available at: www.ahajournals.org/journal/jaha

CLINICAL PERSPECTIVE

What Is New?

- Although serum uric acid (UA) level correlates positively with mean pulmonary arterial pressure, disease severity, and prognosis in patients with pulmonary arterial hypertension, the pathogenic role of UA in the deterioration of pulmonary arterial hypertension remains uncertain.
- In isolated perfused lung preparations, UA induced significantly greater pressor response in the lung with pulmonary hypertension, and was associated with reduced cGMP.
- In pulmonary arterial hypertension rats with hyperuricemia, elevated lung UA was associated with increased right ventricular (RV) afterload and exacerbated occlusive vascular lesions, which were inhibited by blockade of UA transports.

What Are the Clinical Implications?

- The mechanism of increased lung UA may be a novel therapeutic target for pulmonary arterial hypertension complicated with hyperuricemia.

Nonstandard Abbreviations and Acronyms

hPAEC	human pulmonary arterial endothelial cell
Hx	hypoxia
Nx	normoxia
OA	oxonic acid
PAEC	pulmonary arterial endothelial cell
PAH	pulmonary arterial hypertension
RVEDP	right ventricular end-diastolic pressure
RVSP	right ventricular systolic pressure
UA	uric acid
UAT	uric acid transporter
URATv1	voltage-driven urate transporter 1
WT	wild-type
XOR	xanthine oxidoreductase

acetylcholine-stimulated vasodilation in isolated porcine pulmonary arteries.[8] Another study demonstrated that the UA-induced inhibition of NO production was abolished by a uric acid transporter (UAT) inhibitor, benzbromarone, in human umbilical vein endothelial cells.[9] These in vitro studies suggest that UAT-mediated UA increase impairs endothelial function by activating arginase. Considering that endothelial dysfunction, particularly impaired endothelial NO production, plays a critical role in the pathophysiology of PAH,[10] it is possible that UA per se may contribute to the pathogenesis of PAH.

Furthermore, serum level of XOR (xanthine oxidoreductase), the enzyme known to catalyze the oxidation of hypoxanthine to xanthine and xanthine to UA, was significantly elevated in patients with PAH compared with healthy subjects.[11] However, the role of XOR in PAH has not been elucidated. We therefore investigated the roles of UA and XOR in the pathogenesis of PAH.

In the present study, we used VEGF (vascular endothelial growth factor) receptor blockade by a VEGF receptor blocker (SU5416) plus hypoxia/normoxia SU5416/hypoxia/normoxia (SU/Hx/Nx) exposure to establish a rat model of severe PAH, which closely mimics the histology and hemodynamics of PAH in humans. First, we measured gene expression of UATs and UA-induced activation of arginase in cultured human PAECs. Second, we measured the pressor response to UA in perfused lung preparation isolated from SU/Hx/Nx-exposed rats. Third, we examined the impact of UA mediated by UAT on hemodynamics and vascular occlusive lesions in SU/Hx/Nx-exposed PAH rats with hyperuricemia induced by oxonic acid (OA). Finally, we investigated the role of XOR in PAH using SU/Hx/Nx-exposed rats and hypoxia-exposed XOR-knockout mice.

METHODS

The data that support the findings of this study are available from the corresponding author on request.

Animal Experiments

All experimental procedures were approved by the Institutional Animal Care and Use Committee of Kyushu University, Japan, and all animal procedures were performed in compliance with the principles of the National Institutes of Health *Guide for the Care and Use of Laboratory Animals* (National Institutes of Health Publication, Eighth Edition, 2011).

Drugs

SU5416 (Tocris Bioscience) was suspended in carboxymethylcellulose solution (0.5% [wt/vol] carboxymethylcellulose sodium, 0.9% [wt/vol] NaCl, 0.4% [vol/vol] polysorbate, 0.9% [vol/vol] benzyl alcohol in deionized water). OA and benzbromarone were purchased from Tokyo Chemical Industry (Tokyo, Japan). Uric acid and L-norvaline were purchased from Sigma-Aldrich (St. Louis, MO). Topiroxostat (topiro) was purchased from MedChemExpress (Monmouth Junction, NJ).

Human Pulmonary Artery Endothelial Cell Culture

Human PAECs (hPAECs) were purchased from Lonza (Walkersville, MD). The hPAECs were used at passage

5 to 7. Cells were passaged at 70% to 80% confluency, and were cultured in complete endothelial growth medium (EBM-2; Lonza).[12]

UA Stimulation of Cultured hPAECs

The UA solution was prepared as follows: 5.6 mg of UA was added to 4 mL of complete endothelial growth medium (EBM-2) and dissolved completely in a boiling water bath. The final UA concentration was 1.4 mg/mL. The solution was filtered using a filter (pore size=0.22 µm) under a sterile hood to remove microorganisms. The solution was stored at room temperature. Before the experiments, the solution was used to prepare culture medium containing 8 mg/dL of UA. Serum-supplemented medium in cell cultures was replaced with serum-free medium 2 hours before UA stimulation in all the experiments.[12] Human PAECs were cultured with or without UA (8 mg/dL) for 3 or 6 hours. At the end of UA stimulation, the culture medium was collected, and hPAECs were washed with PBS and collected.[8]

Arginase Activity in Cultured hPAECs

Arginase activity was determined by measuring urea content in the culture medium using the QuantiChrom Arginase Assay Kit (BioAssay Systems, Hayward, CA).[13] Cells grown in 6-well plates were incubated in 2 mL of serum-free EBM-2 with or without UA (8 mg/dL), and the urea content in the culture medium was assayed.[8] The medium sample (40 µL) was incubated at 37 °C for 120 minutes in the presence or absence of 10 µL of 5× assay reagent. Urea level was measured, and arginase activity was calculated according to the manufacturer's instructions. The arginase activity in each sample was expressed as U/L.[13]

Rat Model of SU/Hypoxia/Normoxia-Induced Pulmonary Hypertension

Adult male Sprague-Dawley rats (150–200 g; Japan SLC, Hamamatsu, Japan) were given a single subcutaneous injection of a VEGF receptor blocker, SU5416 (20 mg/kg; Tocris Bioscience), and exposed to hypoxia (Hx) (10% O_2) for 3 weeks. They were then returned to normoxia (Nx) for 2 weeks (total of 5 weeks after SU5416 injection).[14] These SU/Hx/Nx rats and normal control rats were used in subsequent experiments. We used male rats because of a more aggressive course of SU/Hx/Nx-induced PAH in male compared with female rats. A total of 218 rats were used, including 46 for isolated perfused lung preparation; 54 for hemodynamic, histology, and immunohistochemistry studies; 24 for reverse transcription-polymerase chain reaction (RT-PCR); and 48 for the measurement of UA level and XOR activity.

Study Using Isolated Perfused Lung Preparations of Rats

This study was performed in normal control and SU/Hx/Nx-exposed rats. The rats were euthanized by an intraperitoneal injection of lethal dose of pentobarbital sodium (30 mg/kg). After an intracardiac injection of 100 IU heparin, the lungs were isolated and ventilated with a humid mixture of 21% O_2, 5% CO_2, and 74% N_2 at a rate of 70 breaths/min with inspiratory and end-expiratory pressures of 10 and 0 cm H_2O, respectively. The lungs were perfused with Earle's Balanced Salt Solution supplemented with 4% (wt/vol) Ficoll, via a pulmonary artery cannula at a constant flow rate of 0.04 mL/min per body weight (grams) using a peristaltic pump.[15] After the blood was flushed from the lungs with 20 mL of perfusate, the lungs were perfused with a total volume of 30 mL of perfusate in a recirculating manner using a closed flow circuit. The effluent from the left ventricle was drained back to the perfusate reservoir. The lung and perfusate temperatures were maintained at 37 °C. The perfusion pressure was continuously monitored with a fluid-filled transducer (DX-300; Nihon Kohden, Tokyo, Japan) as an indication of pulmonary arterial pressure. The left atrial pressure was fixed at 4 mm Hg during measurements by adjusting the height of the outlet tube.

After obtaining a stable recording of baseline perfusion pressure, the pressor responses to bolus injections of angiotensin II (50 ng) and UA (8.4 mg/dL, 500 µmol/L) were examined as reported previously,[8] and 0.5 mL of angiotensin II or UA was prepared in 0.5 mL of perfusate and injected into the flow circuit. The maximum increase in perfusion pressure from baseline was evaluated as the developed pulmonary arterial pressure response.[16] The perfusate was supplemented with 300 µmol/L benzbromarone or 50 mmol/L L-norvaline to examine the effect of UAT or arginase. Benzbromarone (final concentration 300 µmol/L) or L-norvaline (50 mmol/L) was added to the perfusate to examine the effect of UAT or arginase.[17,18]

cGMP Measurement by Enzyme Immunoassay

The protein levels of cGMP in the isolated lung of SU/Hx/Nx-exposed rats without and with treatment with 500 µmol/L of UA were determined by the cGMP enzyme immunoassay (Cayman Chemical, Ann Arbor, MI).[19] A 50-mg sample of frozen lung tissue was homogenized in 0.5 mL 5% (wt/vol) trichloroacetic acid. The supernatant was subjected to trichloroacetic acid extraction using 2.5 mL water-saturated ether 3 times, and the residual ether from the aqueous layer was removed by heating the sample to 70 °C. Next, 50 µL of 5-times diluted samples and standard solutions were incubated with 50 µL of tracer and 50 µL of antibody

at 4 °C overnight. After washing 5 times, plates were incubated with Ellman solution for 2 hours at room temperature with gentle shaking. The plates were read at a wavelength of 412 nm, and the standard curve was produced using the Cayman enzyme immunoassay triple workbook (Cayman Chemical). The sample cGMP concentration was determined (as picomoles per milligram tissue) using the equation obtained from the standard curve.

Rat Model of SU/Hx/Nx-Induced Pulmonary Hypertension With Hyperuricemia

In rodents, UA is degraded by the hepatic enzyme uricase to allantoin. However, mutations in the uricase gene occur during primate development, with the consequence that humans have relatively high serum UA levels.[20] Administration of low doses of a uricase inhibitor, OA, in rats has been reported to induce mild hyperuricemia (1.5- to 2-fold increase in serum UA level) without intrarenal urate crystal deposition leading to acute renal failure.[21] To produce a rat model of SU/Hx/Nx-induced pulmonary hypertension (PH) with hyperuricemia, SU/Hx/Nx-exposed rats were fed a diet containing 2% OA from 1 week before SU5416 injection for 6 weeks (until the end of the protocol).

Experimental Protocols for SU/Hx/Nx-Exposed Rats

Protocol 1: SU/Hx/Nx-Exposed Rats Administered Uricase Inhibitor

A diet containing 2% OA was given to rats from 1 week before injection of SU5416 (week −1) through week 5 after SU5416 injection (Figure 1). Administration of benzbromarone (10 mg/kg, admixed in diet)[22] was started from the day of SU5416 injection to week 5 after injection. The following 4 groups were studied: (1) untreated rats age matched to SU5416-exposed rats (CTRL), (2) SU/Hx/Nx-exposed rats without 2% OA (SU), (3) SU/Hx/Nx-exposed rats with 2% OA (SU/OA), and (4) SU/Hx/Nx and 2% OA-exposed rats with benzbromarone (SU/OA/benzbromarone).

Protocol 2: SU/Hx/Nx-Exposed Rats Not Administered Uricase Inhibitor

Administration of benzbromarone (10 mg/kg, admixed in diet) or topiroxostat (1 mg/kg, admixed in diet)[23] was started from the day of SU5416 injection to week 5. The following 4 groups were studied: (1) untreated rats age matched to rats CTRL, (2) SU rats, (3) SU/Hx/Nx-exposed rats with benzbromarone (SU/benzbromarone), (4) SU/Hx/Nx-exposed rats with topiroxostat (SU/topiro).
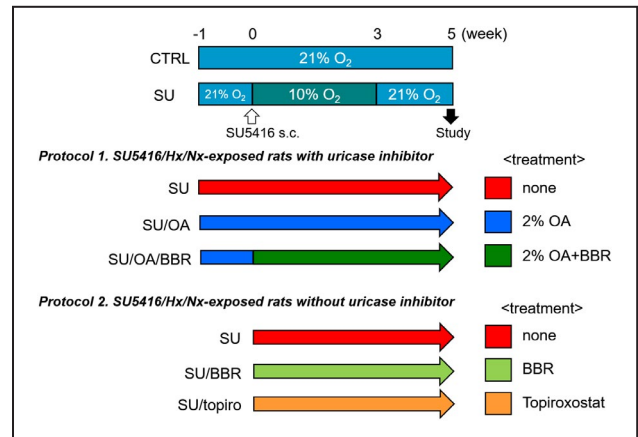

Figure 1. Experimental protocol in SU5416/hypoxia/normoxia-exposed pulmonary hypertension rat model. Protocol 1 aims to examine the effect of hyperuricemia induced by 2% oxonic acid (OA), a uricase inhibitor on SU5416/hypoxia/normoxia (SU/Hx/Nx)-induced pulmonary hypertension (PH), and to examine the effect of uric acid (UA) transporter inhibition by benzbromarone on SU/Hx/Nx-induced PH with hyperuricemia. Protocol 2 aims to examine the effect of UA transporter inhibition by BBR and xanthine oxidoreductase inhibition by topiroxostat on SU/Hx/Nx-induced PH. BBR indicates benzbromarone; CTRL, normal control rat; O2, oxygen; SU, SU5416/hypoxia/normoxia (SU/Hx/Nx)-exposed rat; and topiro, topiroxostat.

At the end of the protocol (week 5), each rat was subjected to hemodynamic evaluation by catheterization. After catheterization, blood was collected from the carotid artery. Then the rat was euthanized by exsanguination under an overdose of isoflurane (2%–5% in room air) and an intraperitoneal injection of lethal dose of pentobarbital sodium (30 mg/kg). The heart was removed for assessment of right ventricular (RV) hypertrophy. RV hypertrophy was expressed as the ratio of RV weight to left ventricle plus septum weight.[14] The lungs were collected for histological evaluation and RT-PCR.

Hemodynamic Evaluation in Rats

At the end of the protocol, rats were anesthetized with isoflurane (induction: 2.5%–3.0% in 1:1 O_2/air mix; maintenance: 1.5%–2.0% in 1:1 O_2/air mix), and attached to a mechanical ventilator (ventilator settings: breathing frequency 110/min, tidal volume 1.5 mL/100 g body weight, inspiratory/expiratory ratio 1:1) via a tracheostomy. Rats were placed on a warming pad to maintain body temperature at 37 °C. An open-chest RV catheterization was performed. A temporary suture was placed around the inferior vena cava, and a needle (23 gauge) puncture in the right ventricle was performed. A microtip P-V catheter (FTH-1912B-8018; Transonic, Ithaca, NY) was inserted into the right ventricle and positioned in the long axis. The signals obtained at steady state (at least 10 seconds) and during temporary inferior vena cava occlusion were

continuously recorded using ML880/9 PowerLab 16/30 (AD Instruments, Dunedin, New Zealand), an ADVantage pressure–volume control unit (v 5.0) (FY097B; Transonic), and a dedicated laboratory computer system. Aortic pressure was measured via the carotid artery using a fluid filled system (DX-360; Nihon-Kohden, Japan). Real-time digital data analysis yielded RV systolic pressure (RVSP), RV end-diastolic pressure (RVEDP), mean aortic pressure, and heart rate.[24]

RV Pressure–Volume Relationships

To obtain multiple pressure–volume loops, we occluded the inferior vena cava to reduce the preload, and determined RV end-systolic pressure and the slope of the end-systolic pressure-volume relationship (end-systolic elastance [Ees]) as a load-independent measurement for RV contractility.[24,25] RV effective arterial elastance (Ea) as a measurement of RV afterload was determined by dividing RV end-systolic pressure by stroke volume of RV. We also obtained RV peak pressures and RVEDP.

Histopathological Analysis

The left lobe of the lung was inflated with PBS containing 1% formalin plus 0.5% agarose via the trachea at a constant pressure of 20 cm H_2O, fixed in 10% formalin neutral buffer solution overnight, and embedded in paraffin. Five-micrometer-thick sections obtained at the level of the hilum were subjected to elastin van Gieson staining and immunohistochemical staining.[14]

Occlusive Lesion of Pulmonary Arteries

All small pulmonary arteries (>100 vessels per cross-section of the left lobe including the hilum, outer diameter [OD] <100 μm) were evaluated. Vessels were assessed for occlusive neointimal lesions on elastin van Gieson–stained sections and scored as follows: no evidence of neointimal formation (grade 0), partial luminal occlusion (<50%, grade 1), and severe luminal occlusion (≥50%, grade 2). Pulmonary artery occlusion rate was expressed as percentage of each grade. The occlusion rates of smaller vessels with OD ≤50 μm and medium sized vessels 50<OD<100 μm were analyzed separately.[26]

Immunohistochemical Study of Arginase Expression

Sections were incubated with primary antibody reactive to arginase I (1:500; No. 610708; BD, Franklin Lakes, NJ)[27] at 4 °C overnight. Sections were then incubated with biotinylated secondary antibody followed by horseradish peroxidase-labeled streptavidin. Pulmonary arteries that appeared to be in a perpendicular cross-section were counted. The intensity of immunostaining was graded semiquantitatively, as described previously.[28] Staining intensity was graded from 0 to 3, with 0 representing the absence of any staining and 3 the maximal intensity. Counted vessels were classified into 2 groups according to smaller vessels with OD ≤50 μm and medium sized vessels 50<OD<100 μm.[26] For each animal, at least 55 vessels were analyzed in a blinded manner.

Analysis of Uric Acid Levels in Plasma and Lung Tissue Using High-Performance Liquid Chromatography

To deproteinize the lung tissues, 20 mg of lung tissue were added to 600 μL of 70% (vol/vol) acetonitrile and homogenized, and the homogenate was centrifuged at 15 000g for 10 minutes at 4 °C. The supernatant was collected and frozen at −80 °C until measurement using high-performance liquid chromatography. Five hundred microliters of plasma was added to 500 μL of 8% (vol/vol) perchloric acid on ice. Six hundred fifty microliters of the mixture was mixed with 40 μL of 2 mol/L K_2CO_3 in 6 mol/L KOH, and centrifuged at 12 000g for 10 minutes at 4 °C. The supernatant was collected and frozen at −80 °C until assay.[29]

Frozen lung tissue extract was dissolved in 80 mmol/L ammonium phosphate buffer (pH 4.1) and filtered through a 0.45-μm filter. Plasma extract was directly measured by high-performance liquid chromatography. High-performance liquid chromatography was performed under the following conditions: instrument, Shimadzu LC-20A High Performance Liquid Chromatography system (Kyoto, Japan); column, YMC-Triart C18 column (25×4.6 mm inner diameter, 3 μm) (Tokyo, Japan); mobile phase, A: 80 mmol/L ammonium phosphate buffer (pH 4.1), B: 30% methanol in A; flow rate, 0.6 mL/min; column temperature at 35 °C; and detector wavelength at 260 nm.[29]

XOR Activity in Lung

XOR activity was measured using the method described previously.[30] In brief, lung homogenate was centrifuged at 105 000g for 60 minutes at 4 °C. These cytosols were added to a mixture containing ($^{15}N_2$)-xanthine (0.8 mmol/L), NAD^+ (1 mmol/L), and oxonate (0.013 mmol/L) in 20 mmol/L Tris buffer (pH 8.5), and incubated at 37 °C for 30 minutes. Then, ($^{13}C_2$, $^{15}N_2$)-UA was added as an internal standard. The mixture was heated for 5 minutes at 95 °C and centrifuged at 15 000g for 10 minutes. The supernatant was filtered through ultrafiltration membrane (Amicons Ultra-0.5 centrifugal filter devices, 3K, Millipore) and ($^{15}N_2$)-UA was measured by liquid chromatography–mass spectrometry (LTQ-Orbitrap). XOR activity was expressed as ($^{15}N_2$)-UA nmol/min per milligram protein.

RT-PCR Analysis

Total RNAs were extracted from hPAECs using the RNeasy Mini Kit (QIAGEN, Hilden, Germany), and mRNA expression level was determined by RT-PCR.[31] The ReverTra Ace qPCR Kit (Toyobo, Tokyo, Japan) and Go Taq Green Master Mix (Promega, Madison, WI) were used for reverse transcription and amplification, respectively. Polymerase chain reaction primers and probes were purchased from TaKaRa Bio. A 10-μL reverse transcription (RT) reaction mixture containing 200 ng of total RNA, oligo dT primer, random primer, and Moloney murine leukemia virus reverse transcriptase was subjected to transverse transcription. An aliquot of RT product was diluted with water, and 150 ng of the complementary DNA (cDNA) was subjected to real-time polymerase chain reaction analysis using Go Taq Green master mix with a polymerase chain reaction system (Applied Biosystems). The thermal cycle consisted of initial denaturation at 94 °C, for 3 minutes, followed by 35 cycles of denaturation at 94 °C for 30 seconds and annealing at 66 °C for 45 seconds and at 72 °C for 45 seconds. Polymerase chain reaction products (10 μL) were separated on 2% (w/v) agarose gels by agarose gel electrophoresis. Table shows the primer sets for individual UATs.

Hypoxia-Induced PH Model Using XOR+/– Mice

XOR+/– mice were kindly gifted by Dr Toshio Ohtsubo. The creation, characterization and genotype of XOR+/– mice have been reported previously.[32] Adult male XOR+/– and wild-type (WT) mice (WT: C57BL6/J; age, 6–7 weeks; body weight, 21–24 g)[32] were exposed to either Nx (room air) or Hx (10% O_2 and 90% N_2) for 3 weeks.[16] A total of 24 mice were used for hemodynamic, histology, RT-PCR, and the measurement of XOR activity.

Mice were anesthetized with isoflurane (induction: 2.5%–3.0%; maintenance: 1.5%–2.0%). A 25-gauge needle connected to a fluid-filled pressure transducer was inserted transthoracically into the right ventricle. Left ventricular systolic pressure (LVSP), RVSP, and heart rate were simultaneously recorded.[16]

Morphometric Analysis of Pulmonary Arterioles in Mice

Lung sections of mice were incubated with primary antibody reactive to α-smooth muscle actin (1:500; M085101; Agilent DAKO, Santa Clara, CA) at 4 °C overnight. Sections were then incubated with biotinylated secondary antibody followed by horseradish peroxidase-labeled streptavidin. Muscularization of pulmonary arterioles 15 to 50 μm in diameter was evaluated based on the degree of histochemical staining of α-smooth muscle actin. Nonmuscular, partially muscular, and totally muscular arterioles were defined by immunostaining of α-smooth muscle actin in <25%, 25% to 75%, and >75%, respectively, of the circumference of the arteriole. At least 60 arterioles were evaluated for each specimen in a blinded manner.[16]

Statistical Analysis

Data are expressed as mean±SEM. One-way ANOVA with Turkey-Kramer post hoc test and Scheffe F test were used for comparisons among the experimental groups. Differences were considered significant at $P<0.05$.

RESULTS

Gene Expression of UA Transporters and Arginase Activity in hPAECs

Among 3 influx (URAT1, urate transporter 1; URATv1, voltage-driven urate transporter 1; and MCT9, monocarboxylic acid transporter 9) and 2 efflux (ABCG2, ATP-binding cassette super-family G member 2; MRP4, multidrug resistance-associated protein 4) transporters, RT-PCR analysis detected mRNA expressions of URATv1, MCT9, ABCG2, and MRP4 in hPAECs (Figure 2A). Arginase activity in hPAECs increased significantly after 3- and 6-hour exposure to 8 mg/dL of UA (Figure 2B).

Pressor Response to UA in Isolated Perfused Lung Preparation of SU/Hx/Nx-Exposed Rats

Isolated lung preparations were used to evaluate the pressor response to UA in the resistance pulmonary

Table 1. Primer Sequences for complementary DNA (cDNA) of Uric Acid Transporters

| Species	cDNA	Reference sequence	Product, bp	Forward Sequence 5′-3′	Reverse Sequence 5′-3′
Human	URAT1	AB071863.1	570	CGGACCTGTATCTCCACGTT	TGCCTTCTTTACTGCCTGGT
	URATv1 (SLC2A9)	AF210317.1	499	GGTGGACTTGTGGGGACATT	CCTCTTGGGAAACGTCTGCT
	ABCG2	AY017168.1	350	GGGTAATCCCCAGGCCTCTA	AGGCATCTGCCTTTGCCTTC
	MRP4 (Abcc4)	AY081219.1	278	TTTTTGACAACGTCCCGCTG	GGTGGTGGGCGTTTCTGATA
	MCT9 (SLC16A9)	NM194298.2	349	CGCTTGGCCTGATTTCAACA	GTGGAAACCCTCCGATGTCAA
Rat	URATv1 (SLC2A9)	NM001191551.1	82	TGGGAACACTGATGGTGAAGATG	GAAATGGCAAATCCGTTGTTGA
	ABCG2	NM181381.2	136	TTTGATAAACGGGGCACCTC	AGCTTTTGGAAGGCGAAGAG
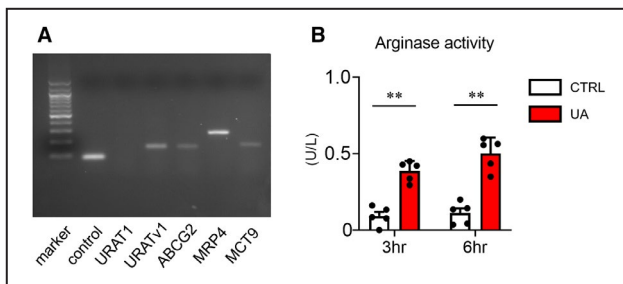
Figure 2. Gene expression of UA transporters and arginase activity in human pulmonary arterial endothelial cells (hPAECs).
A, Representative reverse transcription-polymerase chain reaction results analyzing messenger RNA expression of uric acid transporters in hPAECs. **B**, Effect of UA on arginase activity in the culture medium of hPAECs, measured by ELISA. Data are expressed as mean±SEM, from 5 independent experiments. **$P<0.01$, by 1-way ANOVA followed by Tukey-Kramer post hoc test. ABCG2 indicates ATP-binding cassette super-family G member 2; CTRL, control; MCT9, monocarboxylic acid transporter 9; MRP4, multidrug resistance-associated protein 4; UA, treatment with uric acid (8 mg/dL); URAT1, urate transporter 1; and URATv1, voltage-driven urate transporter 1.

arteries. Baseline perfusion pressure was higher in SU/Hx/Nx-exposed rats than in normal control rats (Figure 3A). In the normal control group, no pressor response to 500 μmol/L of UA was observed despite a moderate response to angiotensin II. In contrast, UA induced significantly greater pressor response in SU/Hx/Nx-exposed rats compared with normal controls. The enhanced pressor response to UA was significantly suppressed by pretreatment with a URATv1 inhibitor, benzbromarone (Figure 3A and 3B). Also, pretreatment with an arginase inhibitor, L-norvaline, significantly reduced the UA-induced pressor response to a similar level as benzbromarone (Figure 3A and 3B).

To determine the effects of UA on NO production, we measured cGMP levels in the isolated lungs of SU/Hx/Nx-exposed rats without and with treatment with 500 μmol/L of UA. UA significantly decreased the level of cGMP in the lungs (Figure 3C).

Chronic Effects of Hyperuricemia on Hemodynamic Parameters in SU/Hx/Nx-Exposed Rats (Protocol 1)

Administration of 2% OA from 1 week before SU5416 injection (week −1) through week 5 after SU5416 injection (SU/OA group) significantly increased UA level in lung tissue compared with normal controls (CTRL group) and SU/Hx/Nx-exposed rats (SU group), and in plasma compared with the CTRL group (Figure 4A and 4B), but did not change XOR activity in the lung (Figure 4C). Administration of benzbromarone (10 mg/kg per day) from the day of SU5416 injection (SU/OA/benzbromarone group) significantly inhibited

OA-induced increase in lung UA level (Figure 4B) but did not affect the increased plasma UA level (Figure 4A). Similar finding was reported previously; benzbromarone did not reduce plasma UA level in Wistar rats administered 2% OA, because urinary excretion rate of UA is higher in rodents than humans, resulting in less predominant urate reabsorption and the lower response to uricosuric agents in rats.[33] There were no significant differences in serum levels of aspartate aminotransferases, alanine aminotransferase, and creatinine among CTRL, SU, SU/OA, and SU/OA/benzbromarone groups (Table S1).

RV pressure-volume curves are shown in Figure 4D. RVSP was significantly elevated in the SU group compared with the CTRL group (Figure 4E). This elevated RVSP in the SU group was significantly accelerated in SU/OA group. There was no significant difference in RVEDP between the SU and SU/OA groups (Figure 4F). RV Ees, a marker of RV contractility, did not differ between the SU and SU/OA groups (Figure 4G), whereas pulmonary Ea, a marker of RV afterload, increased significantly in the SU/OA group (Figure 4H).

Compared with the SU/OA group, RVSP (Figure 4E) was significantly lowered without change in RVEDP (Figure 4F) in the SU/OA/benzbromarone group. Benzbromarone almost normalized Ea (Figure 4H) as well as RVSP without changing Ees (Figure 4G). Mean systemic arterial pressure and heart rate did not differ significantly among the CTRL, SU, SU/OA, and SU/OA/benzbromarone groups (data not shown).

Chronic Effects of Hyperuricemia on Occlusive Lesion Formation in SU/Hx/Nx-Exposed Rats

At 5 weeks after SU5416 injection, the percentage of grade 1 occlusive lesions in smaller pulmonary arteries (OD ≤50 μm) was 56.9%, which was markedly higher than the 5.5% in normal controls (Figure 4I). The percentage of grade 2 occlusive lesions in smaller pulmonary arteries was significantly higher in the SU/OA group compared with the SU group (Figure 4I). Benzbromarone inhibited the increase in percentage of grade 2 occlusive lesions to the same level as in the SU group. In the medium-sized pulmonary arteries (OD: 50–100 μm), grade 2 occlusive lesions were only modestly observed in the SU/OA group (Figure 4I). However, there were no significant differences in percentage of grade 1 occlusive lesions among the SU, SU/OA, and SU/OA/benzbromarone groups (Figure 4I).

Effects of Hyperuricemia on Arginase I Expression in SU/Hx/Nx-Exposed Rats

We assessed a total of 1267 vessels in 23 left lung lobes from 4 groups of rats. Mean numbers of
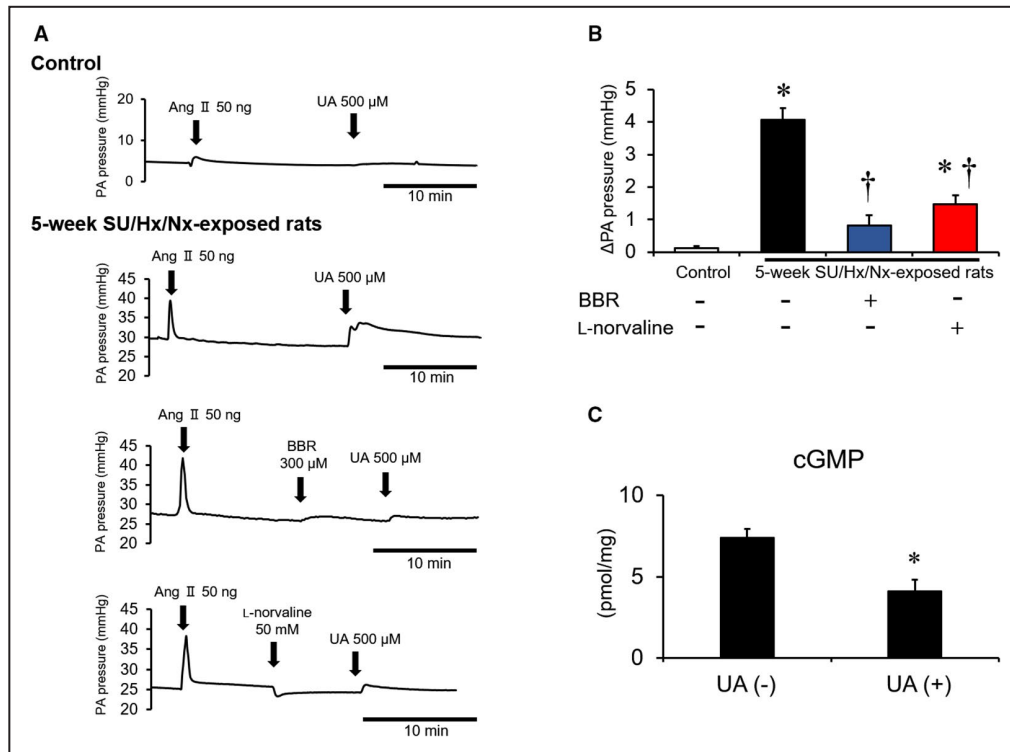
Figure 3. Enhanced pressor response to uric acid (UA) in isolated perfused lung preparations of SU5416/hypoxia/normoxia-exposed pulmonary hypertension rat model.

A, Representative traces of pulmonary arterial pressure (PA pressure) in a perfused lung preparation isolated from age-matched normal control rats (Control) and SU/Hx/Nx-exposed rats at 5 weeks. Angiotensin II (Ang II; 100 ng), benzbromarone (BBR; 300 μmol/L; UA transporter inhibitor), L-norvaline (50 mmol/L; arginase inhibitor), and UA (500 μmol/L) were prepared in 0.5 mL of perfusate and injected into the flow circuit. **B**, Group data of PA pressure increase from baseline (ΔPA pressure) in response to stimulation with UA. Data are expressed as mean±SEM, n=6 to 7. *$P<0.05$ vs control. †$P<0.05$ vs SU/Hx/Nx-exposed rats treated with UA alone, by 1-way ANOVA followed by Scheffe F test. **C**, Levels of cGMP in isolated lung of SU/Hx/Nx-exposed rats without and with treatment with 500 μmol/L of UA. Data are expressed as mean±SEM, n=6. *$P<0.05$ vs without UA, by 1-way ANOVA followed by Scheffe F test.

vessels/lung lobes examined were 55.4, 55.0, 55.0, and 55.0 in CTRL, SU, SU/OA, and SU/OA/benzbromarone groups, respectively. The parenchyma showed no apparent morphologic abnormalities. Immunohistochemical analyses revealed positive immunostaining for arginase I in the innermost

layer of pulmonary arteries in all rats examined (Figure 5A). As shown in Figure 5B, semiquantitative analysis of the immunohistochemical staining indicating arginase I expression in smaller (OD ≤50 μm) and medium-sized (OD: 50–100 μm) pulmonary arteries showed significantly higher grade in the SU

Figure 4. Chronic effects of hyperuricemia in SU5416/hypoxia/normoxia-exposed rats with or without benzbromarone treatment (protocol 1).

A, Uric acid (UA) level in plasma. **B**, UA level in lung tissue measured by high-performance liquid chromatography. **C**, Xanthine oxidoreductase (XOR) activity in lung tissue. Data are expressed as mean±SEM, n=6. *$P<0.05$. **$P<0.01$. **D**, Representative examples of pressure-volume relationship in 4 groups. **E**, Right ventricular (RV) systolic pressure (RVSP). **F**, RV end-diastolic pressure (RVEDP). **G**, RV end-systolic elastance (Ees; a marker of RV contractility). **H**, Pulmonary arterial elastance (Ea; a marker of RV afterload). Data are expressed as mean±SEM, n=5 to 8. *$P<0.05$. **$P<0.01$. **I**, Representative low magnification photomicrographs of Verhoeff-van Gieson stained lung sections (upper panels). Scale bars of upper panels indicate 200 μm. Arrowheads indicate occlusive pulmonary arteries (PAs). Insets show higher magnification photomicrographs of PAs. Pulmonary arterial occlusion is scored as grade 0 (no luminal occlusion; white), grade 1 (<50% occlusion; grey), and grade 2 (≥50% occlusion; black) (lower panels). Scale bars of lower panels indicate 50 μm. The graph shows percentage of occlusive PAs with outer diameter (OD) ≤50 μm and 50<OD<100 μm. Data are expressed as mean±SEM, n=7 to 8. *$P<0.05$. **$P<0.01$ vs CTRL. †$P<0.05$ and ‡$P<0.01$ vs SU. #$P<0.05$ and ##$P<0.01$ vs SU/OA, by 1-way ANOVA followed by Tukey-Kramer post hoc test. BBR indicates benzbromarone, a UA transporter inhibitor; CTRL, normal control rat; ns, not significant, by 1-way ANOVA followed by Tukey-Kramer post hoc test; OA, oxonic acid; SU/OA/BBR, SU/Hx/Nx-exposed rat administered 2% OA and benzbromarone; SU/OA, SU/Hx/Nx-exposed rat administered 2% OA; and SU, SU5416/hypoxia/normoxia (SU/Hx/Nx)-exposed rat.
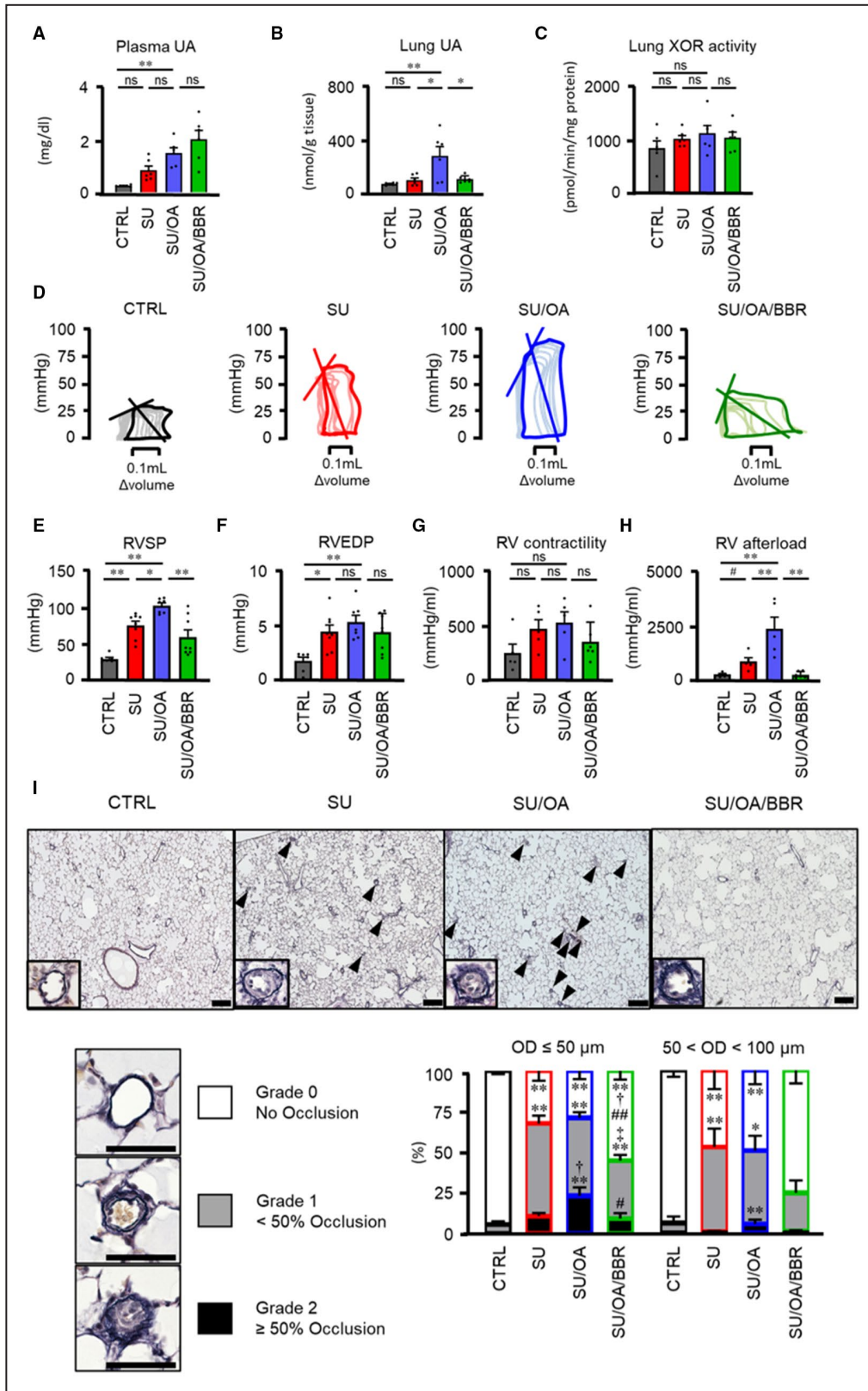
group compared with the CTRL group. The arginase I expression increased further in the SU/OA group in smaller pulmonary arteries, whereas there was no significant increase in medium-sized pulmonary arteries. Administration of benzbromarone normalized the OA-induced increase of arginase I expression in both smaller- and medium-sized pulmonary arteries.
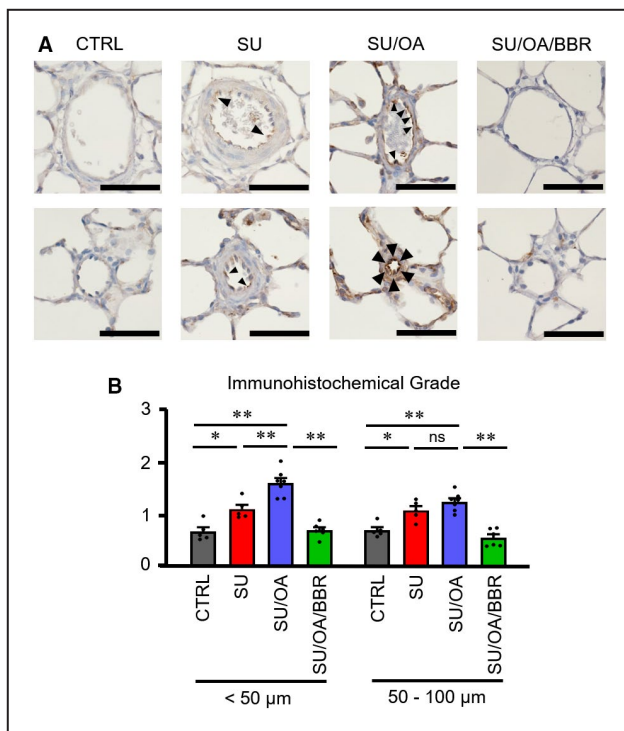
Figure 5. Immunoreactivity of arginase in pulmonary arteries in SU5416/hypoxia/normoxia-exposed rats with or without benzbromarone treatment.

A, Representative photomicrographs of arginase I-immunostained pulmonary arteries (upper panels: medium sized arteries 50–100 μm in OD, lower panels: smaller arteries ≤50 μm in OD). Arrowheads indicate arginase I-positive cells. Scale bars indicate 50 μm. **B**, Bars indicate grade of arginase I immunoreactivity in the innermost layer of smaller (≤50 μm) and medium sized (50–100 μm) pulmonary arteries. Scoring of immunohistochemical grade is described in the Methods section. Data are expressed as mean±SEM, n=5 to 7. *$P<0.05$. **$P<0.01$. BBR indicates benzbromarone; CTRL, normal control rat; ns, not significant, by 1-way ANOVA followed by Tukey-Kramer post hoc test; OA, oxonic acid; SU/OA/BBR, SU/Hx/Nx-exposed rat administered 2% OA and benzbromarone; SU/OA, SU/Hx/Nx-exposed rat administered 2% OA; and SU, SU5416/hypoxia/normoxia (SU/Hx/Nx)-exposed rat.

Role of Xanthine Oxidoreductase in SU5416/Hx/Nx-Exposed Rats (Protocol 2)

Plasma and lung UA levels did not differ between the CTRL and SU groups (Figure 6A and 6B), whereas lung XOR activity increased significantly in the SU group compared with the CTRL group (Figure 6C). Benzbromarone (10 mg/kg per day) did not suppress lung XOR activity in the SU/benzbromarone group (Figure 6C). On the other hand, topiroxostat (1 mg/kg per day) reduced lung XOR activity in the SU/topiro group (Figure 6C). There were no significant differences in serum levels of aspartate aminotransferases, alanine aminotransferase, and creatinine among the CTRL, SU, SU/benzbromarone, and SU/topiro groups (Table S2).

The RV pressure-volume curves are shown in Figure 6D. RVSP was significantly elevated in the SU group (Figure 6E) compared with the CTRL group. There was no significant difference in RVEDP (Figure 6F) between the CTRL and SU groups. Topiroxostat as well as benzbromarone did not suppress RVSP, RVEDP, Ees, or Ea in SU/Hx/Nx-exposed rats. Mean systemic arterial pressure and heart rate did not significantly differ among the CTRL, SU, SU/benzbromarone, and SU/topiro groups (data not shown).

At 5 weeks after SU5416 injection, the percentage of grade 1 occlusive lesions in smaller pulmonary arteries (OD ≤50 μm) increased significantly compared with normal controls (44.4% versus 17.9%) (Figure 6I). Benzbromarone and topiroxostat did not inhibit the increase in percentage of grade 2 occlusive lesions in SU/Hx/Nx-exposed rats.

Effects of Knockout of XOR Gene on Hemodynamic Parameters and Arteriolar Muscularization in Hypoxia-Induced PH in Mice

The role of XOR in the development of PH was further corroborated using XOR+/− mice. Exposure of WT mice to 10% O$_2$ hypoxia for 3 weeks significantly elevated XOR activity (Figure 7A), increased RVSP (Figure 7B), and induced RV hypertrophy (Figure 7C) compared with a normoxic condition. Hypoxia had no significant effect on the LVSP or heart rate in WT mice (data not shown). Under normoxic conditions, RVSP and RV hypertrophy were comparable in XOR+/− mice

Figure 6. Chronic effects of benzbromarone or topiroxostat in SU5416/hypoxia/normoxia-exposed rats without hyperuricemia (protocol 2).

A, Uric acid (UA) levels in plasma. **B**, UA levels in lung tissues measured by high-performance liquid chromatography. **C**, Xanthine oxidoreductase (XOR) activity in lung tissues. Data are expressed as mean±SEM, n=6. *$P<0.05$. **$P<0.01$. **D**, Representative examples of pressure-volume relationship in 4 groups. **E**, Right ventricular (RV) systolic pressure (RVSP). **F**, RV end-diastolic pressure (RVEDP). **G**, RV end-systolic elastance (a marker of RV contractility). **H**, pulmonary arterial elastance (a marker of RV afterload). Data are expressed as mean±SEM, n=5 to 8. **$P<0.01$. #$P<0.05$. **I**, Representative low magnification photomicrographs of Verhoeff-van Gieson stained lung sections (upper panels). Scale bars of upper panels indicate 200 μm. Arrowheads indicate occlusive pulmonary arteries (PAs). Insets show higher magnification photomicrographs of PAs. Pulmonary arterial occlusion is scored as grade 0 (no luminal occlusion; white), grade 1 (≤50% occlusion; grey), and grade 2 (≥50% occlusion; black) (lower panels). Scale bars of lower panels indicate 50 μm. Percentage of occlusive PAs with OD ≤50 μm (left) and 50<OD<100 μm (right). Data are expressed as mean±SEM, n=5 to 8. *$P<0.05$. **$P<0.01$ vs CTRL. †$P<0.05$ vs SU, by 1-way ANOVA followed by Tukey-Kramer post hoc test. BBR indicates benzbromarone; CTRL, normal control rat; ns, not significant, by 1-way ANOVA followed by Tukey-Kramer post hoc test; OA, 2% oxonic acid; SU, SU5416/hypoxia/normoxia (SU/Hx/Nx)-exposed rat; SU/BBR, SU/Hx/Nx-exposed rat administered benzbromarone; SU/topiro, SU/Hx/Nx-exposed rat administered topiroxostat; and topiro, topiroxostat.
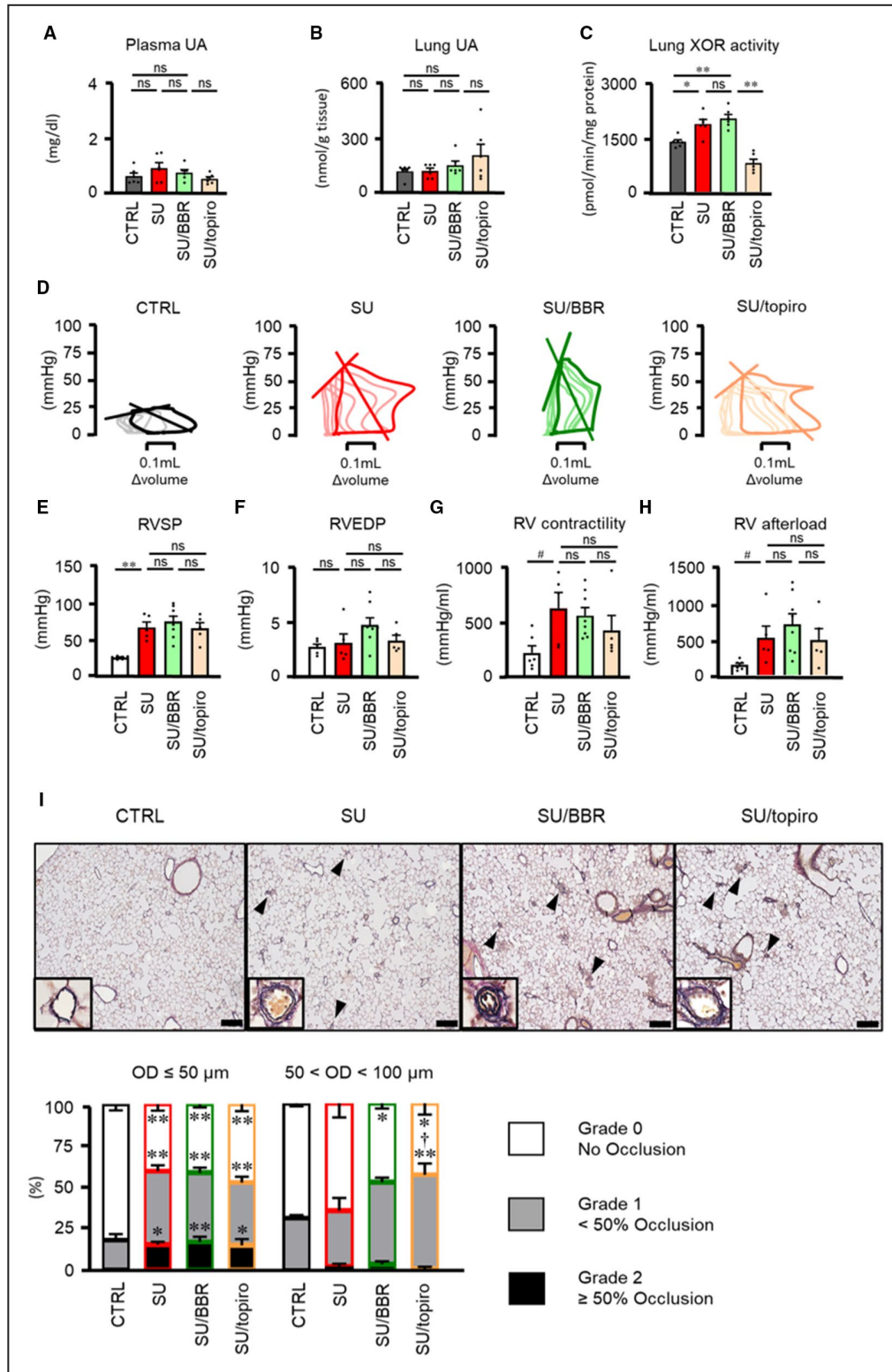
and WT mice (Figure 7B and 7C). When XOR+/− mice were exposed to hypoxia for 3 weeks, the degrees of RVSP elevation and RV hypertrophy development did not differ between WT and XOR+/− mice (Figure 7B and 7C). Hypoxia had no significant effect on LVSP and heart rate in XOR+/− mice (data now shown).

Muscularization of pulmonary arterioles is another manifestation of vascular remodeling in PH observed in arterioles with diameters of 15 to 50 μm. Histochemical detection of α-smooth muscle actin and quantitative analysis of the percentage of the circumferential length showing positive staining revealed a significant
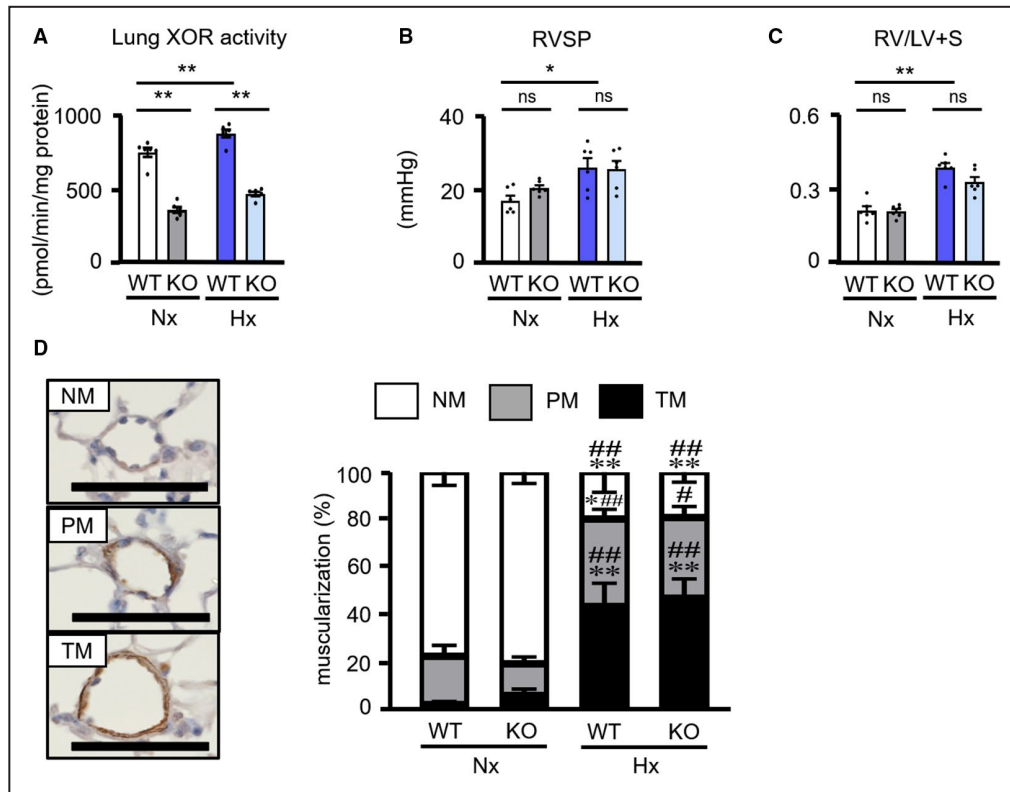
Figure 7.   Effects of xanthine oxidoreductase (XOR)-knockout on hemodynamic parameters and arteriolar muscularization in hypoxia-induced pulmonary hypertension (PH) mice model.
This protocol aims to examine the effects of XOR on hypoxia-induced PH. **A**, XOR activity in lung tissue. Data are expressed as mean±SEM, n=6. **P<0.01, by 1-way ANOVA followed by Tukey-Kramer post hoc test. **B**, Right ventricular (RV) systolic pressure (RVSP). **C**, Right ventricle weight to (left ventricle [LV]+septum [S]) weight (RV/LV+S) ratio in WT-Nx, KO-Nx, WT-Hx, and KO-Hx groups. Data are expressed as mean±SEM, n=6. *P<0.05. **P<0.01. D, (Left) Representative photomicrographs showing immunohistochemical staining of α-smooth muscle actin in pulmonary arterioles graded as nonmuscular (NM), partially muscular (PM), and totally muscular (TM). (Right) Group data of muscularization of pulmonary arterioles in WT-Nx, KO-Nx, WT-Hx, and KO-Hx mice. NM, PM, and TM were defined as positive immunostaining in <25%, 25% to 75%, and >75% of the circumference of the arteriole, respectively. The percentage of TM, PM, and NM was analyzed statistically. Scale bars indicate 50 μm. Data are expressed as mean±SEM, n=6. *P<0.05 and **P<0.01 vs WT-Nx. #P<0.05 and ##P<0.01 vs KO-Nx, by 1-way ANOVA followed by Tukey-Kramer post hoc test. Hx indicates mice exposed to 10% O_2 hypoxia for 3 weeks; KO, age-matched XOR+/− mice; ns, not significant, by 1-way ANOVA followed by Tukey-Kramer post hoc test; Nx, mice housed under normoxic conditions; and WT, age-matched wild-type mice.

increase in percentage of partially and totally muscularized arterioles in WT mice after exposure to hypoxia, which indicated increased muscularization of pulmonary arterioles (Figure 7D). Hypoxia-induced muscularization of pulmonary arterioles did not differ between WT and XOR+/− mice.

DISCUSSION

The major findings of the present study are as follows: (1) In perfused lungs isolated from SU/Hx/Nx-exposed rats, UA decreased cGMP level, a surrogate marker of NO production, and induced greater pressor response, which was suppressed by arginase inhibitor and UAT blockade with benzbromarone. (2) SU/Hx/Nx-exposed

rats with hyperuricemia showed elevated lung UA level, deteriorated PH, and marked occlusive lesion formation, which were prevented by benzbromarone. These findings indicate that increased lung UA level mediated by UAT plays a critical role in the progression of PAH (Figure 8).

Endothelial damage and the accompanying decrease in endogenous NO production are generally considered to contribute to deterioration of PAH.[34] In healthy subjects, serum UA and serum NO levels show opposite circadian rhythms, and the timing of peak UA and trough NO concentrations was virtually synchronous.[35] In addition, a recent study demonstrated that UA reduced NO production by activating arginase in porcine PAECs.[8] Consistent with previous findings, the present study demonstrated that
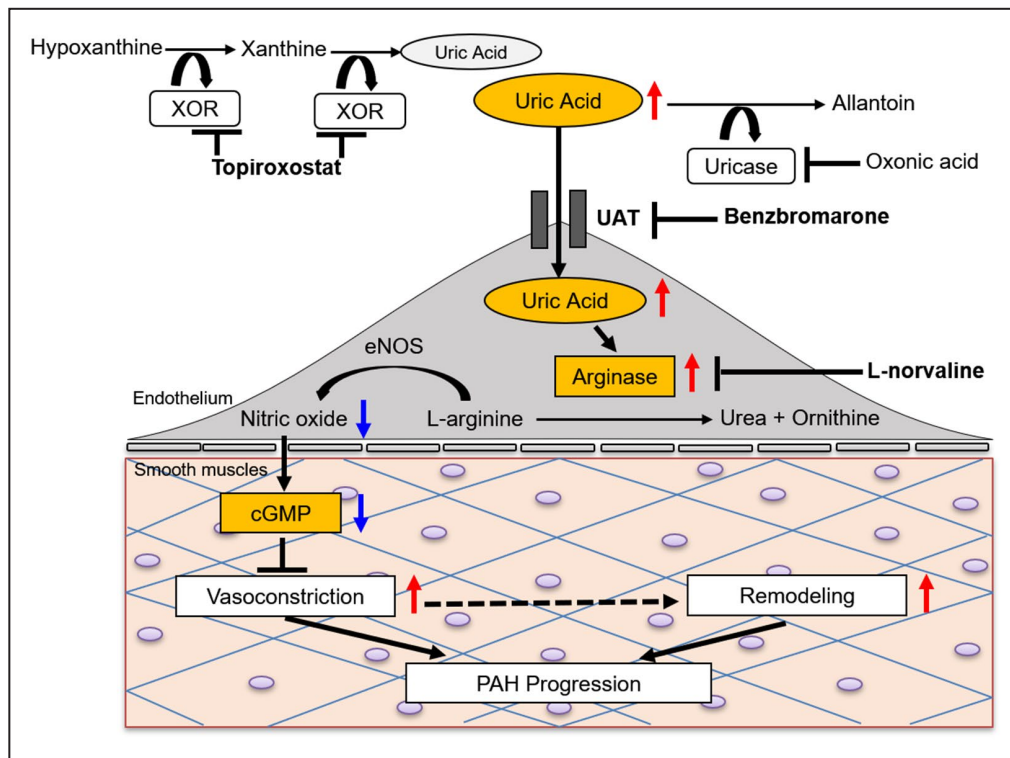
Figure 8.   Schematic illustration of the involvement of uric acid in the development of pulmonary arterial hypertension in SU5416/hypoxia/normoxia-exposed rats.
eNOS indicates endothelial NO synthase; PAH, pulmonary arterial hypertension; UAT, uric acid transporter; and XOR, xanthine oxidoreductase.

treatment with UA induced arginase activation in hPAECs (Figure 2B), and that UA decreased cGMP levels in the isolated lungs of SU/Hx/Nx-exposed rats (Figure 3C). Furthermore, UA-induced pressor response was completely suppressed by pretreatment with an arginase inhibitor in SU/Hx/Nx-exposed rats (Figure 3A and 3B). These data suggest that UA may decrease endothelial NO production by activating arginase in PAECs, consequently increasing pulmonary vascular resistance (PVR) in PAH rats. Our previous study in SU/Hx/Nx-exposed rats showed that although NO bioavailability was impaired in the early phase of PAH, it was restored and even enhanced over time as PAH progressed, and the restored endothelial NO activity moderated severe pulmonary vasoconstriction to keep RVSP and PVR at lower levels.[36] We also demonstrated that ρ-kinase–mediated vasoconstriction contributed markedly to the high RVSP and PVR throughout the PAH process from the early (1 week) to late (13 weeks) phase in SU/Hx/Nx-exposed rats.[26] These findings lead to the speculation that UA-induced decrease in endogenous NO unmasks the sustained vasoconstriction to further elevate RVSP and PVR. We have recently reported that hemodynamic stress plays a critical role in the development and maintenance of perivascular inflammation and neointimal lesions in SU/Hx/Nx-exposed rats.[31,37] It is therefore possible that elevated RVSP and PVR by decreased NO may

further develop occlusive lesions in SU/Hx/Nx-exposed rats with hyperuricemia (Figure 8). In the present study, it remains unclear how the NO-mediated mechanism is responsible for the development of neointimal lesions in SU/Hx/Nx-exposed rats with hyperuricemia, although immunohistochemical study revealed high arginase I expression in the innermost layer of occlusive pulmonary arteries (Figure 5). Further study is needed to investigate how increased UA chronically aggravates neointimal lesion formation throughout the PAH process.

On UATs, particularly influx transporter, URATv1 protein expression has been demonstrated in cultured PAECs isolated from idiopathic patients with PAH.[6] We detected mRNA expressions of URATv1 and MCT9 in cultured human PAECs (Figure 2A) and URATv1 in the rat lung (Figure 9). Considering that benzbromarone did not influence the activity of MCT9 in human umbilical vein endothelial cells,[9] it is possible that benzbromarone inhibits URATv1 under hyperuricemic condition and blocks the transportation of UA into the lungs. However, the lung UA level and UAT profiling in patients with PAH remain unknown. Further study is needed to identify which UAT plays the major role in the intracellular transportation of UA throughout the PAH process. Benzbromarone was also reported to block the
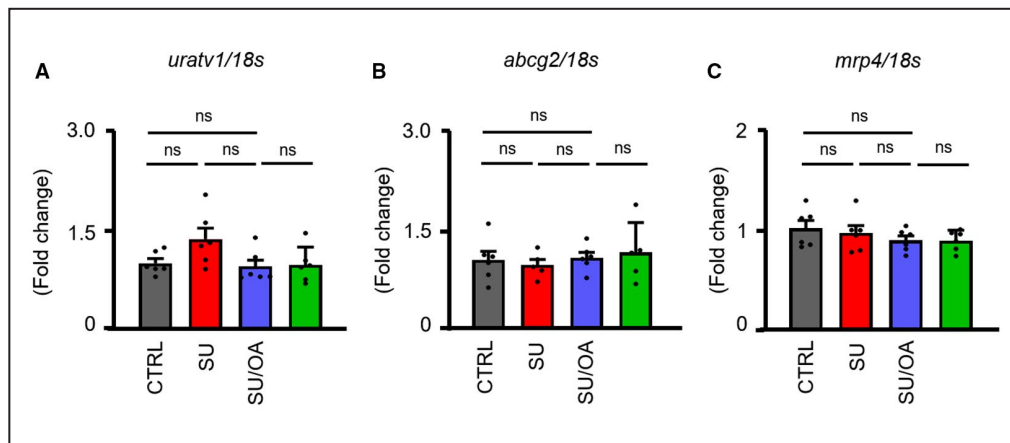
Figure 9. Quantification of urate transporter genes in SU5416/hypoxia/normoxia-exposed rats with or without benzbromarone or topiroxostat.

Messenger RNA expression level of *uratv1* (**A**), *abcg2* (**B**), and *mrp4* (**C**) in the lung measured by reverse transcription-polymerase chain reaction. Data are expressed as mean±SEM, n=6. 18s, 18s ribosomal RNA; *abcg2* indicates ATP-binding cassette super-family G member 2; BBR, benzbromarone; CTRL, normal control rat; *mrp4*, multidrug resistance-associated protein 4; ns, not significant, by 1-way ANOVA followed by Tukey-Kramer post hoc test; OA, oxonic acid; SU/OA/BBR, SU/Hx/Nx-exposed rat with 2% OA and benzbromarone; SU/OA, SU/Hx/Nx-exposed rat with 2% OA; SU, SU5416/hypoxia/normoxia (SU/Hx/Nx)-exposed rat; and *uratv1*, voltage-driven urate transporter 1.

Ca²⁺-activated Cl⁻ channel transmembrane protein 16A (TMEM16A).[38] Recent studies demonstrated that chronic treatment with benzbromarone partially reverses PH in both hypoxia-exposed mice and monocrotaline-exposed rats without hyperuricemia, through inhibition of TMEM16A.[18] In cultured pulmonary artery smooth muscle cells from PAH lung, benzbromarone normalized membrane potential and blocked platelet-derived growth factor-induced proliferation, suggesting that benzbromarone not only blocks UAT blockade but exhibits multiple modes of action.[18] In our study, benzbromarone had no beneficial effects on PH and occlusive lesions in SU/Hx/Nx-exposed rats without hyperuricemia (Figure 6). Therefore, it is conceivable that benzbromarone prevents the deterioration of PAH under hyperuricemic conditions by targeting and inhibiting UATs, whereas other targets of benzbromarone may not play a significant role in the PAH process.

Administration of benzbromarone (10 mg/kg per day) from the day of SU5416 injection (SU/OA/benzbromarone group) did not affect the increased plasma UA level (Figure 4A). The inhibition of UATs in renal tubules is expected to facilitate the urinary excretion of UA, therefore leading to decrease in plasma UA level. On the other hand, the inhibition of UATs that contribute to cellular UA uptake may result in an increase in the plasma level of UA. The urinary reabsorption of UA is a major determinant of the plasma level of UA in humans. In this human situation, administration of benzbromarone is expected to decrease the plasma UA level because of the dominant effect of inhibition

of renal UA reabsorption, compared with that of cellular UA uptake, on the plasma UA level. In contrast, the rodents exhibit greater urinary excretion rate of UA than in humans, presumably because of lower activity of renal reabsorption.[33] Therefore, the effect of benzbromarone administration on the plasma UA level would be subject to the balance between inhibition of renal absorption and inhibition of cellular uptake. As a result, the plasma UA level may not be much influenced after benzbromarone administration in the rodents.

UA has been reported to induce inflammation including IL-1β (interleukin-1β) and ICAM-1 (intercellular adhesion molecule 1) production through activation of the nucleotide-binding domain and leucine-rich repeat-containing receptors family pyrin domain containing 3 (NLRP3) inflammasome in human umbilical vein endothelial cells.[39] The activation of NLRP3 inflammasome was observed in the whole lung of hypoxia-exposed mice and monocrotaline-exposed rats, and its activation induced pulmonary artery smooth muscle cell proliferation in hypoxia-exposed mice.[40,41] Exposure to UA significantly induced proliferation of cultured pulmonary artery smooth muscle cells isolated from idiopathic patients with PAH.[6] However, monocrotaline-exposed rats treated with OA did not develop significant medial wall thickening.[6] Consistent with this recent study, we observed no further progression of media thickening despite the development of occlusive lesions in SU/Hx/Nx-exposed rats administered 2% OA compared with SU/Hx/Nx-exposed rats not administered 2% OA (data not shown). These findings suggest that the

effect of UA on the progression of media thickening in the rat PH model is relatively minor.

On the effect of UA on the myocardium, myocardial infarction model rats with hyperuricemia showed decreased left ventricular contractility because of myocardial hypertrophy and increased fibrosis.[22] In our study, there was no significant change in the index of RV contractility (Ees) between 2% OA-treated and untreated SU/Hx/Nx-exposed rats, whereas the index of RV afterload (Ea) was significantly higher in SU/Hx/Nx-exposed rats administered 2% OA compared with 2% OA-untreated SU/Hx/Nx-exposed rats. These results suggest that UA contributes mainly to the exacerbation of pulmonary vascular resistance and does not contribute to RV contractility in PAH.

XOR, an important enzyme that converts purines to xanthine and UA,[42] has been known to be an important source of reactive oxygen species in various cardiovascular diseases.[43] Previous studies reported improvement of pulmonary vascular remodeling by the XOR inhibitor allopurinol in a hypoxia-induced PH mouse model.[44,45] On the other hand, it is possible that XOR may protect against PH development because it is a potent source of NO under hypoxic conditions.[46] Thus, the role of XOR in PAH remains controversial. In the present study, XOR activity increased significantly in SU/Hx/Nx-exposed lungs compared with control lungs, whereas there was no significant difference in lung tissue XOR activity between 2% OA-treated and untreated SU/Hx/Nx-exposed rats (Figure 4C). However, reduction of lung XOR activity by topiroxostat failed to improve PH and pulmonary vascular remodeling in SU/Hx/Nx-exposed rats (Figure 6). Furthermore, in the hypoxia-induced PH model, there were no differences in the increased RVSP and pulmonary vascular remodeling between WT and XOR-knockout mice (Figure 7). Although XOR activity is lower in humans than rodents,[47] an observational study indicated elevated serum XOR activity in patients with PAH compared with healthy subjects.[11] Considering our results that pharmacological and genetic XOR inhibitions had no effect on the development of PAH in rodent PH models, it is conceivable that XOR per se does not contribute to the deterioration of PAH (Figure 8).

In conclusion, we demonstrated that UA directly plays a critical role in the pathogenesis and progression of PAH, whereas XOR had no such effect in rodent PH models. In PAH lung preparation, UA decreased cGMP level and increased PVR, and the PVR response was abolished by arginase and UAT inhibitors. In PAH rats with hyperuricemia, elevated lung UA level deteriorated hemodynamics and exacerbated occlusive vascular lesions, which were inhibited by blockade of UAT. These observations provide insight for the development of novel therapeutic strategies for PAH complicated with

hyperuricemia by targeting the UATs. However, there is no epidemiological study that investigated the effect of benzbromarone on hemodynamics and clinical outcome in patients with PAH with hyperuricemia. The clinical usefulness of UAT blockade by benzbromarone remains to be investigated in future clinical studies. In addition, it remains unknown which UAT mainly contributes to UA transportation into pulmonary vasculature and deterioration of PAH. Further investigations are needed to determine the specific UAT involved in PAH development, and to examine whether inhibition of the specific UAT effectively and safely prevents deterioration in PAH patients with hyperuricemia.

REFERENCES

1. Tuder RM, Abman SH, Braun T, Capron F, Stevens T, Thistlethwaite PA, Haworth SG. Development and pathology of pulmonary hypertension. *J Am Coll Cardiol*. 2009;54:S3–S9. doi: 10.1016/j.jacc.2009.04.009

2. Christman BW, McPherson CD, Newman JH, King GA, Bernard GR, Groves BM, Loyd JE. An imbalance between the excretion of thromboxane and prostacyclin metabolites in pulmonary hypertension. *N Engl J Med*. 1992;327:70–75. doi: 10.1056/NEJM199207093270202

3. Galie N, Manes A, Branzi A. The endothelin system in pulmonary arterial hypertension. *Cardiovasc Res*. 2004;61:227–237. doi: 10.1016/j.cardiores.2003.11.026

4. Humbert M, Sitbon O, Chaouat A, Bertocchi M, Habib G, Gressin V, Yaici A, Weitzenblum E, Cordier J-F, Chabot F, et al. Pulmonary arterial hypertension in France: results from a national registry. *Am J Respir Crit Care Med*. 2006;173:1023–1030. doi: 10.1164/rccm.200510-1668OC

5. Nagaya N, Uematsu M, Satoh T, Kyotani S, Sakamaki F, Nakanishi N, Yamagishi M, Kunieda T, Miyatake K. Serum uric acid levels correlate with the severity and the mortality of primary pulmonary hypertension. *Am J Respir Crit Care Med*. 1999;160:487–492. doi: 10.1164/ajrccm.160.2.9812078

6. Savale L, Akagi S, Tu LY, Cumont A, Thuillet R, Phan C, Le Vely B, Berrebeh N, Huertas A, Jaïs X, et al. Serum and pulmonary uric acid in pulmonary arterial hypertension. *Eur Respir J*. 2021;58:2000332. doi: 10.1183/13993003.00332-2020

7. Voelkel MA, Wynne KM, Badesch DB, Groves BM, Voelkel NF. Hyperuricemia in severe pulmonary hypertension. *Chest*. 2000;117:19–24. doi: 10.1378/chest.117.1.19

8. Zharikov S, Krotova K, Hu H, Baylis C, Johnson RJ, Block ER, Patel J. Uric acid decreases no production and increases arginase activity in cultured pulmonary artery endothelial cells. *Am J Physiol Cell Physiol*. 2008;295:C1183–C1190. doi: 10.1152/ajpcell.00075.2008

9. Mishima M, Hamada T, Maharani N, Ikeda N, Onohara T, Notsu T, Ninomiya H, Miyazaki S, Mizuta E, Sugihara S, et al. Effects of uric acid on the no production of HUVECs and its restoration by urate lowering agents. *Drug Res (Stuttg)*. 2016;66:270–274. doi: 10.1055/s-0035-1569405

10. Budhiraja R, Tuder RM, Hassoun PM. Endothelial dysfunction in pulmonary hypertension. *Circulation*. 2004;109:159–165. doi: 10.1161/01.CIR.0000102381.57477.50

11. Spiekermann S, Schenk K, Hoeper MM. Increased xanthine oxidase activity in idiopathic pulmonary arterial hypertension. *Eur Respir J*. 2009;34:276. doi: 10.1183/09031936.00013309

12. Ghosh S, Gupta M, Xu W, Mavrakis DA, Janocha AJ, Comhair SAA, Haque MM, Stuehr DJ, Yu J, Polgar P, et al. Phosphorylation inactivation of endothelial nitric oxide synthesis in pulmonary arterial hypertension. *Am J Physiol Lung Cell Mol Physiol*. 2016;310:L1199–L1205. doi: 10.1152/ajplung.00092.2016

13. Monin L, Griffiths KL, Lam WY, Gopal R, Kang DD, Ahmed M, Rajamanickam A, Cruz-Lagunas A, Zúñiga J, Babu S, et al. Helminth-induced arginase-1 exacerbates lung inflammation and disease severity in tuberculosis. *J Clin Invest*. 2015;125:4699–4713. doi: 10.1172/JCI77378

14. Abe K, Toba M, Alzoubi A, Ito M, Fagan KA, Cool CD, Voelkel NF, McMurtry IF, Oka M. Formation of plexiform lesions in experimental severe pulmonary arterial hypertension. *Circulation*. 2010;121:2747–2754. doi: 10.1161/CIRCULATIONAHA.109.927681

15. Oka M, Ohnishi M, Takahashi H, Soma S, Hasunuma K, Sato K, Kira S. Altered vasoreactivity in lungs isolated from rats exposed to nitric oxide gas. *Am J Physiol*. 1996;271:L419–L424. doi: 10.1152/ajplung.1996.271.3.L419

16. Kuwabara Y, Tanaka-Ishikawa M, Abe K, Hirano M, Hirooka Y, Tsutsui H, Sunagawa K, Hirano K. Proteinase-activated receptor 1 antagonism ameliorates experimental pulmonary hypertension. *Cardiovasc Res*. 2019;115:1357–1368. doi: 10.1093/cvr/cvy284

17. Ming XF, Rajapakse AG, Carvas JM, Ruffieux J, Yang Z. Inhibition of S6K1 accounts partially for the anti-inflammatory effects of the arginase inhibitor L-norvaline. *BMC Cardiovasc Disord*. 2009;9:12. doi: 10.1186/1471-2261-9-12

18. Papp R, Nagaraj C, Zabini D, Nagy BM, Lengyel M, Skofic Maurer D, Sharma N, Egemnazarov B, Kovacs G, Kwapiszewska G, et al. Targeting TMEM16A to reverse vasoconstriction and remodelling in idiopathic pulmonary arterial hypertension. *Eur Respir J*. 2019;53:1800965.

19. Lang M, Kojonazarov B, Tian X, Kalymbetov A, Weissmann N, Grimminger F, Kretschmer A, Stasch J-P, Seeger W, Ghofrani HA, et al. The soluble guanylate cyclase stimulator riociguat ameliorates pulmonary hypertension induced by hypoxia and SU5416 in rats. *PLoS One*. 2012;7:e43433. doi: 10.1371/journal.pone.0043433

20. Wu XW, Muzny DM, Lee CC, Caskey CT. Two independent mutational events in the loss of urate oxidase during hominoid evolution. *J Mol Evol*. 1992;34:78–84. doi: 10.1007/BF00163854

21. Mazzali M, Hughes J, Kim YG, Jefferson A, Kang DH, Gordon KL, Lan YL, Kivlighn S, Johnson RJ. Elevated uric acid increases blood pressure in the rat by a novel crystal-independent mechanism. *Hypertension*. 2001;38:1101–1106. doi: 10.1161/hy1101.092839

22. Chen CC, Hsu YJ, Lee TM. Impact of elevated uric acid on ventricular remodeling in infarcted rats with experimental hyperuricemia. *Am J Physiol Heart Circ Physiol*. 2011;301:H1107–H1117. doi: 10.1152/ajpheart.01071.2010

23. Kawamorita Y, Shiraishi T, Tamura Y, Kumagai T, Shibata S, Fujigaki Y, Hosoyamada M, Nakagawa T, Uchida S. Renoprotective effect of topiroxostat via antioxidant activity in puromycin aminonucleoside nephrosis rats. *Physiol Rep*. 2017;5:e13358. doi: 10.14814/phy2.13358

24. da Silva Gonçalves Bós D, Van Der Bruggen CEE, Kurakula K, Sun X-Q, Casali KR, Casali AG, Rol N, Szulcek R, dos Remedios C, Guignabert C, et al. Contribution of impaired parasympathetic activity to right ventricular dysfunction and pulmonary vascular remodeling in pulmonary arterial hypertension. *Circulation*. 2018;137:910–924. doi: 10.1161/CIRCULATIONAHA.117.027451

25. Kono A, Maughan WL, Sunagawa K, Hamilton K, Sagawa K, Weisfeldt ML. The use of left ventricular end-ejection pressure and peak pressure in the estimation of the end-systolic pressure-volume relationship. *Circulation*. 1984;70:1057–1065. doi: 10.1161/01.CIR.70.6.1057

26. Toba M, Alzoubi A, O'Neill KD, Gairhe S, Matsumoto Y, Oshima K, Abe K, Oka M, McMurtry IF. Temporal hemodynamic and histological progression in Sugen5416/hypoxia/normoxia-exposed pulmonary arterial hypertensive rats. *Am J Physiol Heart Circ Physiol*. 2014;306:H243–H250. doi: 10.1152/ajpheart.00728.2013

27. Jung C, Grün K, Betge S, Pernow J, Kelm M, Muessig J, Masyuk M, Kuethe F, Ndongson-Dongmo B, Bauer R, et al. Arginase inhibition reverses monocrotaline-induced pulmonary hypertension. *Int J Mol Sci*. 2017;18:1609. doi: 10.3390/ijms18081609

28. Giaid A, Saleh D. Reduced expression of endothelial nitric oxide synthase in the lungs of patients with pulmonary hypertension. *N Engl J Med*. 1995;333:214–221. doi: 10.1056/NEJM199507273330403

29. Kaneko K, Aoyagi Y, Fukuuchi T, Inazawa K, Yamaoka N. Total purine and purine base content of common foodstuffs for facilitating nutritional therapy for gout and hyperuricemia. *Biol Pharm Bull*. 2014;37:709–721.

30. Ohata K, Kamijo-Ikemori A, Sugaya T, Hibi C, Nakamura T, Murase T, Oikawa T, Hoshino S, Katayama K, Asano J, et al. Renoprotective effect of the xanthine oxidoreductase inhibitor topiroxostat under decreased angiotensin II type 1a receptor expression. *Eur J Pharmacol*. 2017;815:88–97. doi: 10.1016/j.ejphar.2017.09.005

31. Abe K, Shinoda M, Tanaka M, Kuwabara Y, Yoshida K, Hirooka Y, McMurtry IF, Oka M, Sunagawa K. Haemodynamic unloading reverses occlusive vascular lesions in severe pulmonary hypertension. *Cardiovasc Res*. 2016;111:16–25. doi: 10.1093/cvr/cvw070

32. Ohtsubo T, Rovira II, Starost MF, Liu C, Finkel T. Xanthine oxidoreductase is an endogenous regulator of cyclooxygenase-2. *Circ Res*. 2004;95:1118–1124. doi: 10.1161/01.RES.0000149571.96304.36

33. Taniguchi T, Ashizawa N, Matsumoto K, Iwanaga T, Saitoh K. Uricosuric agents decrease the plasma urate level in rats by concomitant treatment with topiroxostat, a novel xanthine oxidoreductase inhibitor. *J Pharm Pharmacol*. 2016;68:76–83. doi: 10.1111/jphp.12490

34. Moncada S, Palmer RM, Higgs EA. Nitric oxide: physiology, pathophysiology, and pharmacology. *Pharmacol Rev*. 1991;43:109–142.

35. Kanabrocki EL, Third JL, Ryan MD, Nemchausky BA, Shirazi P, Scheving LE, McVormick JB, Hermida RC, Bremner WF, Hoppensteadt DA, et al. Circadian relationship of serum uric acid and nitric oxide. *JAMA*. 2000;283:2240–2241. doi: 10.1001/jama.283.17.2235

36. Tanaka M, Abe K, Oka M, Saku K, Yoshida K, Ishikawa T, McMurtry IF, Sunagawa K, Hoka S, Tsutsui H. Inhibition of nitric oxide synthase unmasks vigorous vasoconstriction in established pulmonary arterial hypertension. *Physiol Rep*. 2017;5:e13537. doi: 10.14814/phy2.13537

37. Kuebler WM, Nicolls MR, Olschewski A, Abe K, Rabinovitch M, Stewart D, Chan SY, Morrell NW, Archer SL, Spiekerkoetter E. A pro-con debate: current controversies in PAH pathogenesis at the American Thoracic Society International Conference in 2017. *Am J Physiol Lung Cell Mol Physiol*. 2018;315:L502–L516. doi: 10.1152/ajplung.00150.2018

38. Huang F, Zhang H, Wu M, Yang H, Kudo M, Peters CJ, Woodruff PG, Solberg OD, Donne ML, Huang X, et al. Calcium-activated chloride channel TMEM16A modulates mucin secretion and airway smooth muscle contraction. *Proc Natl Acad Sci USA*. 2012;109:16354–16359. doi: 10.1073/pnas.1214596109

39. Yin W, Zhou QL, OuYang SX, Chen Y, Gong YT, Liang YM. Uric acid regulates NLRP3/IL-1beta signaling pathway and further induces vascular endothelial cells injury in early CKD through ROS activation and K(+) efflux. *BMC Nephrol*. 2019;20:319.

40. Cero FT, Hillestad V, Sjaastad I, Yndestad A, Aukrust P, Ranheim T, Lunde IG, Olsen MB, Lien E, Zhang L, et al. Absence of the inflammasome adaptor ASC reduces hypoxia-induced pulmonary hypertension in mice. *Am J Physiol Lung Cell Mol Physiol*. 2015;309:L378–L387. doi: 10.1152/ajplung.00342.2014

41. Tang B, Chen GX, Liang MY, Yao JP, Wu ZK. Ellagic acid prevents monocrotaline-induced pulmonary artery hypertension via inhibiting NLRP3 inflammasome activation in rats. *Int J Cardiol*. 2015;180:134–141. doi: 10.1016/j.ijcard.2014.11.161

42. Hille R, Nishino T. Xanthine oxidase and xanthine dehydrogenase. *FASEB J*. 1995;9:995–1003. doi: 10.1096/fasebj.9.11.7649415

43. Tsutsui H, Kinugawa S, Matsushima S. Oxidative stress and heart failure. *Am J Physiol Heart Circ Physiol*. 2011;301:H2181–H2190. doi: 10.1152/ajpheart.00554.2011

44. Hoshikawa Y, Ono S, Suzuki S, Tanita T, Chida M, Song C, Noda M, Tabata T, Voelkel NF, Fujimura S. Generation of oxidative stress contributes to the development of pulmonary hypertension induced by hypoxia. *J Appl Physiol*. 2001;90:1299–1306. doi: 10.1152/jappl.2001.90.4.1299

45. Jankov RP, Kantores C, Pan J, Belik J. Contribution of xanthine oxidase-derived superoxide to chronic hypoxic pulmonary hypertension in neonatal rats. *Am J Physiol Lung Cell Mol Physiol*. 2008;294:L233–L245. doi: 10.1152/ajplung.00166.2007

46. Zuckerbraun BS, Shiva S, Ifedigbo E, Mathier MA, Mollen KP, Rao J, Bauer PM, Choi JJW, Curtis E, Choi AMK, et al. Nitrite potently inhibits hypoxic and inflammatory pulmonary arterial hypertension and smooth muscle proliferation via xanthine oxidoreductase-dependent nitric oxide generation. *Circulation*. 2010;121:98–109. doi: 10.1161/CIRCULATIONAHA.109.891077

47. de Yong JW, van der Meer P, Nieukoop AS, Huizer T, Stroeve RJ, Bos E. Xanthine oxidoreductase activity in perfused hearts of various species, including humans. *Circ Res*. 1990;67:770–773. doi: 10.1161/01.RES.67.3.770

Supplemental Material

Table S1. Body weight, right ventricular hypertrophy, and blood tests (protocol 1).

	Control	SU	SU/OA	SU/OA/BBR
Body and heart weights				
N	7	8	7	8
Body weight, g	333 ± 16	271 ± 11 *	237 ± 16 **	229 ± 13 **
RV weight, mg	144 ± 8	413 ± 37 **	311 ± 58	257 ± 38
LV+S weight, mg	611 ± 24	630 ± 37	517 ± 61	504 ± 35
RVH	0.23 ± 0.01	0.65 ± 0.05 **	0.57 ± 0.05 **	0.50 ± 0.06 **
Blood test				
N	7	8	7	8
Cr, mg/dL	0.43 ± 0.04	0.56 ± 0.05	0.52 ± 0.05	0.42 ± 0.04
AST, U/L	92 ± 13	150 ± 11	121 ± 15	137 ± 22
ALT, U/L	48 ± 6	49 ± 4	44 ± 5	48 ± 6

BW: body weight; RV: right ventricular; LV+S: left ventricle plus septum: Cr: creatinine; AST: aspartate aminotransferase; ALT: alanine aminotransferase; CTRL: control; SU: SU5416/hypoxia/normoxia; OA: oxonic acid; BBR: benzbromarone. Data are expressed as mean ± SEM, n = 7-8. * $p < 0.05$ and ** $p < 0.01$ vs. CTRL, by one-way ANOVA followed by Tukey-Kramer post hoc test.

Table S2. Body weight, right ventricular hypertrophy, and blood tests (protocol 2).

	CTRL	SU		SU/BBR		SU/topiro	
Body and heart weights							
N	6	5		8		5	
Body weight, g	346 ± 4	281 ± 15	**	302 ± 8		282 ± 17	*
RV weight, mg	166 ± 5	409 ± 34	**	445 ± 25	**	381 ± 38	**
LV+S weight, mg	666 ± 14	638 ± 12		720 ± 31		682 ± 21	
RVH	0.25 ± 0.01	0.64 ± 0.06	**	0.62 ± 0.03	**	0.56 ± 0.04	**
Blood test							
N	6	5		8		5	
Cr, mg/dL	0.36 ± 0.02	0.41 ± 0.02		0.43 ± 0.03		0.39 ± 0.02	
AST, U/L	79 ± 13	114 ± 26		125 ± 18		92 ± 12	
ALT, U/L	37 ± 6	41 ± 6		43 ± 6		40 ± 2	

BW: body weight; RV: right ventricular; LV+S: left ventricle plus septum; Cr: creatinine; AST: aspartate aminotransferase; ALT: alanine aminotransferase; CTRL: control; SU: SU5416/hypoxia/normoxia; BBR: benzbromarone; topiro: topiroxostat. Data are expressed as mean ± SEM, n = 5-8. * $p < 0.05$ and ** $p < 0.01$ vs. control, by one-way ANOVA followed by Tukey-Kramer post hoc test.